Al-Farouk journal of sciences
Volume (2), Issue (5) (Nov, 2026)
ISSN: 3135-2359

مجلة الفاروق للعلوم
المجلد (2) العدد 5 نوفمبر 2026
عدد خاص بالمؤتمر العلمي الرابع للعلوم والتقنية
28-29 نوفمبر 2026 مصراتة – ليبيا
إدارة المعاهد العليا – وزارة التعليم التقني

Adsorption of Méthylène Blue from its Aqueous Solution Using Chemically Modified Tea Leaves Residue

Mawahib M. Abousnena
The Libyan Academy-Trpoli-Libya
mmbk1888@gmail.com

Received: 29/7/2026 Revised: 20/8/2026 Accepted: 28/8/2026 Publication: 28/11/2026

Abstract

The textile dyeing industry is one of the largest contributors to the production of enormous quantities of dye-contaminated water. Removing this type of pollutant is a major concern for environmentalists due to its dangers to the environment and public health.

In this study, the effectiveness of chemically modified tea leaves residue (MTLR) was investigated. This residue was treated with sodium hydroxide (NaOH) solution to remove methylene blue (MB) dye from its aqueous solution. A series of batch-mode experiments were conducted to test the effect of (0.15-0.50 g) of MTLR adsorbent at pH levels of (3.0–10), contact times of (5–90 min), and (50–300 mg/l) concentrations of MB adsorbent in a 50 ml solution.

The results demonstrated a good adsorption capacity (q) for MB, with equilibrium being achieved within approximately 30 min. for various MB concentrations. Furthermore, adsorption was found to increase with increasing mass of MTLR, and rising pH up to 7.0; the optimal initial concentration was identified at 150 mg/l under the specified operating conditions. Additionally, the experimental findings aligned well with the Langmuir isotherm model, exhibiting a linear regression value (R^2) of 0.970. The maximum monolayer adsorption capacity (q_{max}) of the chemically modified adsorbent toward MB, evaluated via the Langmuir model, was found to be 13.265 mg/g. This represents a distinct enhancement compared to the capacity of 10.34 mg/g achieved prior to NaOH treatment. Consequently, MTLR serves as a more effective adsorbent for MB removal than the raw untreated residue.

Keywords: adsorption, single batch system, methylene blue dye, modified tea leaf residue, isotherm models.

1. Introduction

For several decades, those concerned with environmental issues have been grappling with the problem of environmental pollution, especially in light of the technological advancements accompanying modern life. Environmental pollution has become a global concern. Pollution, in all its various forms, affects the aquatic environment (surface water and groundwater) as a result of the mixing of water with colored organic materials such as dyes. This causes an imbalance in the proportions of the basic components of the aquatic environment, deviating from their natural levels. This often occurs due to human interference or certain natural phenomena [1].

Water pollution is a very serious problem, as water is a fundamental and essential component for the survival of all life forms. Paper printing plants, agricultural fertilizers, paints, plastics manufacturing, and leather and textile tanning are among the most significant sources of dye wastewater. Leather and textile tanning plants are the largest of these industries, generating enormous quantities of wastewater laden with manufacturing byproducts, particularly dyes. Generally, manufacturing facilities face major challenges in finding effective wastewater treatment solutions. The indiscriminate discharge of industrial wastewater is unacceptable due to its negative impacts as most industrial dyes are highly toxic to aquatic life [2].

Therefore, pollution control and management has become a top priority in recent years, and providing clean water for various activities remains one of the greatest challenges that researchers around the world are aiming to address. In this regard, a number of technologies have been developed and implemented to remove natural pollutants such as dyes from water, including (1) physical

technologies such as adsorption, membrane separation, reverse osmosis, and ion exchange; (2) chemical technologies such as catalytic reduction, coagulation, chemical oxidation, and ozonolysis; and (3) biological technologies such as bacterial remediation via aerobic/anaerobic environments and algae remediation [3–5]. Research and innovation teams believe these technologies are reasonably good, but each has varying degrees of success. Moreover, all of the above-mentioned technologies, with the exception of adsorption, are often ineffective in reducing pollutant concentrations to the desired level and are complex in design and costly [6, 7]. Finding another, more effective technology that is superior to those mentioned above was a priority and essential to ensuring the quality and safety of the aquatic environment. Over time, attempts have continued to find the optimal, most effective, and cost-efficient method for treating polluted water. In several countries, particularly developing nations, adsorption technologies have been observed to be the best option due to their ease of design and operation, low cost, effectiveness, and relatively short processing time compared to other technologies [8, 9].

In an effort to make treatment more economically viable, researchers have sought cheaper adsorbents than activated carbon, sourced from agricultural and food waste. Examples of green adsorbents published in several scientific journals include olive leaves [10]. Pine leaves [11], almond shells [12], orange peels [13], olive pits [14], date pits [15], used coffee grounds [16], and tea leaf residue (TLR) [17] are all examples of agricultural waste.

Tea is the most consumed beverage after drinking water, as evidenced by the annual production of tea leaves, estimated at approximately 7 million tons according to the Food and Agriculture Organization of the United Nations (FAO) in 2022 [18]. After brewing, the tea leaves become residue and are classified as agricultural solid waste. This waste is often disposed of by dumping it in open areas or burning it, causing negative environmental impacts.

This study aims to evaluate the efficiency of chemically modified MTLR as an adsorbent material in removing MB from aqueous solution using batch mode adsorption in laboratory experiments. The study also seeks to mitigate the problem of indiscriminate disposal of TLR. The effects of several physical variables on the adsorption process were investigated, including the concentration of MB, the mass of the MTLR, pH, and contact time.

2. Equipment, Tools, and Working Methods

2.1 Equipment and Tools

In this study, several instruments were used, most importantly a Fourier transform infrared (FT-IR) spectroscopy to determine the functional groups present in the structures of unmodified TLR in the range of (400–4000 cm^{-1}). The spectrometer used was the TENSORP-27 model, manufactured in Germany by BRUKER. Then, a UV/visible spectrophotometer, a Speccord 205 model (UV-Analytikjena, Germany), to measure the concentrations of MB at a wavelength of λ = 665 nm. Next, a pH meter, the Inolab 740 model (WTW model), was used with a SenTix 20 pH model double electrode. Finally, a digital vibrator, the GFL 3005 model (Germany), was used for the batch mode adsorption study.

2.2 Chemicals

For batch mode adsorption studies, commercial-grade MB dye (91% purity, BDH Chemicals Ltd., England) and analytical-grade NaOH (5.0%, Riedel-De Haën, Germany), used for adsorbent modification, were acquired. The adsorbent, unmodified TLR (originally from Sri Lanka), was obtained from a local vendor. All solutions were prepared using double-distilled water.

2.3 Preparation Processes

2.3.1 Preparation of Chemically Modified Tea Leaves Residue (MTLR)

Chemical modification of adsorbents significantly enhances their maximum capacity by expanding the proportion of active surface areas [19]. Crucially, this treatment stabilizes tannin compounds within the matrix, preventing their leaching into the aqueous phase during processing. This inhibition is essential, as the release of tannins can discolor the water and subsequently elevate the chemical oxygen demand (COD) [20]. Furthermore, alkaline modification effectively strips away non-cellulosic constituents, such as lipids and waxes, from the lignocellulosic fiber surfaces, thereby exposing key oxygen-containing functional groups—particularly hydroxyl (-OH) groups [21].

In this study, the raw material consisting of TLR was treated by immersion in a 0.5 M NaOH solution for 5 hours, followed by thorough washing with distilled water, and then oven drying at 105°C

for 24 hours. Finally, the residue was ground manually, sieved, and its particle size was measured to be approximately 400 µm.

2.3.2 Methylene Blue (MB): Specifications and Stock Solutions Preparation

Chemically, methylene blue (MB) is designated as the 3,7-bis(dimethyl-amino) phenolthiazin-5-ium chloride cation. Table 1 shows the chemical formula, molecular weight, and chemical composition of the dye, along with some other chemical properties.

Table (1): Properties and specifications of methylene blue dye (MB) [22]

Common Name	Methylene blue
Chemical Formula	$C_{16}H_{18}ClN_3S.3H_2O$
Molecular Weight (g/mol)	373.9
Molecular Volume (cm^{-1}/mol)	241.9
Diameter of Molecule	0.8
Maximum Wavelength (λ_{max})	668
Chromatic Index	52.015
Chemical Structure	

The stock standard solution of MB dye (1000 mg/l) was prepared by dissolving the exact weight of the dye in distilled water. Subsequently, working solutions with diverse dye concentrations were generated through appropriate dilution of the stock solution using distilled water.

2.3.4 Batch-Mode Adsorption Process

In this study, adsorption was performed using a digital shaker at a constant shaking rate of 170 rpm, at a room temperature of (25±2 °C), for varying contact times (5–90 min). at pH levels between (3-10), using 250 ml conical flasks. All adsorption processes involved mixing different masses of TLR, ranging from (0.15-0.50 g), with 50 mL solutions containing varying initial dye concentrations (50–300 mg/l). After adsorption, the residual concentrations of MB in each conical flask were determined spectroscopically after filtering the contents of each flask using Whatman filter paper.

Equation (1) illustrates how to estimate the amount of adsorption at equilibrium, (qe) expressed in mg/g, as follows:

$$qe = ((Co - Ce) * V)) / m \quad ... \quad (1)$$

Where: the variables (C_o) and (C_e) (mg/l) represent the liquid phase concentrations of the dye at the beginning and end of the adsorption process, respectively; (V), measured in liters, represents the volume of the dye solution; and (W) measured in grams, represents the mass of the adsorbent used in the adsorption process.

Conversely, Equation (2) illustrates how to estimate the percentage of adsorption (%) as follows:

$$\%\,\text{Adsorption} = ((Co - Ce) / Co) * 100 \quad ... \quad (2)$$

This study evaluated the effects of several physical parameters on the adsorption process, namely the initial MB dye concentration, MTLR adsorbent mass, contact time, and pH.

2.2.5 Equilibrium Adsorption Isotherm Study

The isotherm aims to describe in detail the relationship between the amount of adsorbed material on the adsorbent at equilibrium. This description is then expressed as the adsorption capacity (q) as a function of the concentration of the adsorbent liquid (C_e) at a constant temperature [23]. Therefore, studying the isotherm is crucial for obtaining accurate data used to design a good and efficient adsorption process [24].

There are several models for isotherm adsorption, but the Langmuir and Freundlich models are the most common and widely used [25]. In fact, important information about the adsorption mechanism, the surface properties of the adsorbent, and its affinity can be obtained from the isotherm equations of adsorption [26].

In the first model, Langmuir assumes a specific homogeneous type of adsorption. That is, when one molecule of the adsorbent occupies a specific active site on the adsorbent particles, no other

molecule can occupy the same active site. This can be illustrated by the following equation (3) [27, 28].

$$qe = qmax\, KL\, Ce / (1 + KLCe) \quad . \; . \; . \quad (3)$$

Where: (qe) represents the solid-phase concentrations of the adsorbent along with the adsorbed material molecules at equilibrium, and is measured in mg/g, (q_{max}) represents the maximum adsorption capacity and is measured in mg/g, (C_e) represents the adsorbed material concentrations at equilibrium and is measured in mg/l, (K_L) represents the value of the Langmuir constant and is measured in l/mg, and the linear representation can be written as follows (4):

$$Ce / qe = 1 / (qmax\, .b) + (1 / qmax)\, Ce \quad . \; . \; . \quad (4)$$

On the other hand, many study results showed that the concentrations on the adsorbent are often exponentially proportional to the concentrations of the residual (unadsorbed) substance to be adsorbed in the solution. Freundlich thus established this relationship in his own model, which assumes that adsorption occurs on heterogeneous surfaces of the adsorbent (Not a homogenous surfaces as in Langmuir model) and that the adsorption capacity is related to the concentrations of the adsorbent at equilibrium, as shown in Equation (5) [27, 28]:

$$qe = KF\, Ce^{(1/n)} \quad . \; . \; . \quad (5)$$

Where: (qe) represents the solid-phase concentrations of the adsorbent and the adsorbed material at equilibrium and is measured in mg/g, while (C_e) represents the liquid-phase concentrations (the adsorbed material remaining in solution) at equilibrium and is measured in mg/l, while (K_F) represents the Freundlich adsorption capacity constant (it indicates the affinity of the adsorbent for the adsorbate); the unit (K_F) is not fixed, as it mathematically depends on the exponent value. The term (1/n) serves as the heterogeneity factor, while, (n) denotes the adsorption intensity constant, which indicates the overall strength of the adsorption process. The Freundlich model can be written linearly as follows (6):

$$\log qe = \log KF + (1/n) \log Ce \quad . \; . \; . \quad (6)$$

3. Results and Discussion

3.1 FT-IR Spectroscopic Analysis and Surface Functionality Comparison of Raw Tea Leaves Residue (TLR) and Modified Tea Leaves Residue (MTLR)

(I) Characterization of Raw Tea Leaves Residue (TLR)

The raw unmodified TLR was thoroughly washed with hot water to ensure the complete removal of impurities and residual color, **if any,** repeating the process several times until the material was virtually colorless. Next, the tea leaves were washed several times with distilled water and air-dried for 24 hrs. Finally, the TLR was oven-dried at 105 °C for 24 hours [29]. The residue was then hand-ground, sieved, and its particle size was measured to be approximately 400 µm.

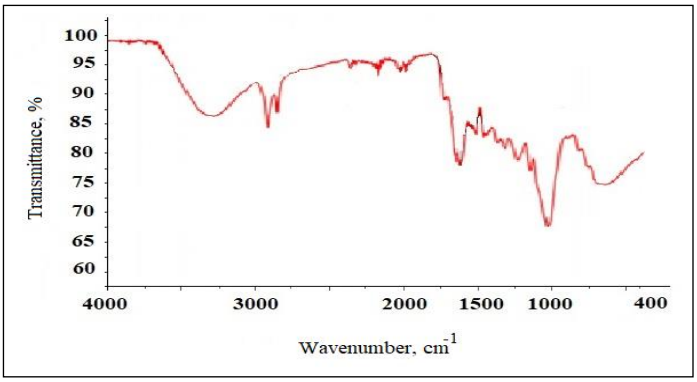


Figure 1: FT-IR Spectrum of the tea leaves residue (TLR) as an unmodified raw material.

A quantity of ground TLR was used as a raw material and analyzed by Fourier transform infrared spectroscopy (FT-IR) to determine the functional groups present in its chemical structure within the range of (4000–400 cm^{-1}). Figure 1 illustrates the FT-IR spectrum of the unmodified TLR. A distinct broad band is observed at 3310 cm^{-1}, which corresponds to the H-bonded hydroxyl group (-OH) stretching vibrations present in cellulose and polyphenolic compounds [29, 30]. The spectrum also reveals another weak band with a shoulder at a wavenumber of 2920 cm^{-1}, indicating the presence of (C-H) stretching vibrations in the aliphatic chains [31]. Another prominent band appears at approximately 1625 cm^{-1}, which is primarily attributed to the conjugated carbonyl (>C=O) stretching or

aromatic ring (C=C) stretching vibrations characteristic of the lignin and tannin frameworks [30, 32, 33]. Furthermore, the figure shows small peaks at wavenumbers between approximately 1400 cm^{-1} and 1520 cm^{-1}, resulting from the (N–H) bending/deformation vibrations of the amide (II) group [34]. Finally, the absorption band at a wavenumber of 1035 cm^{-1} is indicative of the (C–O) stretching vibration in alcohols and cellulose structures [35]. Therefore, it can be concluded that the FT–IR analysis of TLR confirmed the primary presence of hydroxyl (–OH) and carbonyl (>C=O) groups, which are likely responsible for the adsorption and bonding processes with MB via specific chemical interactions."

(II) Characterization of Modified Tea Leaves Residue (MTLR)

Generally, substances such as cellulose, hemicellulose, lignin, proteins, fatty acids, and amino acids are often among the chemical structures of agricultural materials, and therefore they are also among the components of used unmodified TLR. They contain functional groups (such as hydroxyl, carboxyl, etc.) which can be effective adsorbents and removers for a number of pollutants from various aquatic environments [36].

One study [37] indicated that the content of the raw TLR in terms of chemical compositions and their abundance ratios consists of proteins of about (14.43%), fats (4.44%), total carbohydrates fibers (50–60%), total ash (4.94%), crude fibers (plant cell wall fibers) (33.63%) and moisture (3.20%).

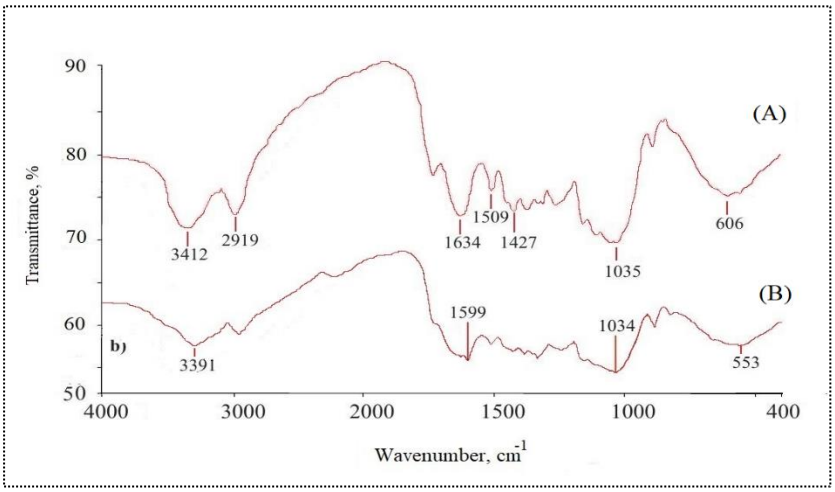


Figure 2: FT–IR spectrum of (MTLR) (A) before adsorption, (B) after adsorption.

Figure 2A displays the Fourier transform infrared (FT–IR) spectrum of the MTLR before MB adsorption within the (4000–400 cm^{-1}) region. Compared to the raw material, significant modifications are evident in the characteristic functional group peaks due to the NaOH treatment. The most prominent feature of the MTLR spectrum is the strong, broad absorption band centered at approximately 3412 cm^{-1}, which corresponds to the stretching vibrations of either the isolated hydroxyl groups (–OH) present in cellulose, lignin, and pectin structures (alcohols, phenols, and carboxylic acids), the amine groups ($-NH_2$), or a combination of both [38 – 41].

Additionally, the spectrum reveals an intermediate peak at approximately 2919 cm^{-1}, attributed to aliphatic (C–H) stretching vibrations in the cellulosic matrix [42]. Another distinct absorption band is observed at 1634 cm^{-1}, which can be assigned to either the extended carbonyl (>C=O) stretching of amide (I) groups [43] or C=C stretching in the aromatic rings of phenolic compounds [44]. The subsequent peak at approximately 1509 cm^{-1} is likely representative of the aromatic skeletal vibrations, primarily associated with lignin [45]. The shoulder at roughly 1427 cm^{-1} is ascribed to the deformation bending of methylene groups ($-CH_2-$) in alkanes [46] or O–H bending in carboxylic acids. The strong broad band at 1035 cm^{-1} is indicative of (C–O) stretching in alcohols (C–OH) or (C–H) stretching in the aromatic structures of cellulose, hemicellulose, and pectin [47, 48]. These initial baseline characteristics confirm that the alkaline treatment effectively "activates" the raw adsorbent by removing surface impurities and enriching the availability of hydroxyl (–OH) and carboxyl (–COOH) reactive sites, which will most often be responsible for the adsorption and bonding processes with MB molecules through one of the adsorption mechanisms as elsewhere [49].

In comparison, Figure 2B presents the FT–IR spectrum of the MTLR matrix after MB adsorption. Following dye uptake, the spectrum displays distinct structural modifications and systematic alterations in peak intensities—both enhancements and reductions—along with significant wavenumber shifts

between the pre-adsorption and post-adsorption states. These specific variations clearly demonstrate that the dye immobilization process directly involved active surface groups, particularly the hydroxyl (-OH), carbonyl (>C=O), and carboxyl (-COOH) functionalities, which served as binding sites to trap MB molecules. Ultimately, these dynamic chemical interactions firmly corroborate that the adsorption process proceeds via a chemisorption pathway, mediated by hydrogen bonding, ion exchange, and electrostatic attractions [50, 51].

3.2 The Effect of pH

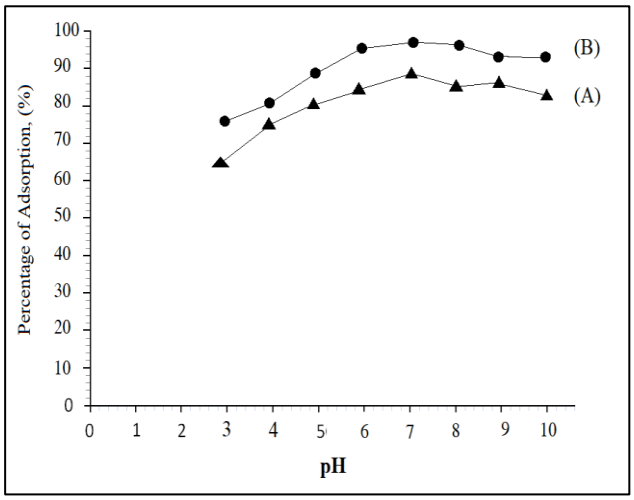


Figure (3): The effect of pH on the adsorption rate (%) of (MB) by (A) (TLR) and (B) (MTLR).

pH is a key factor during the adsorption process, affecting the surface charge of the adsorbent, the degree of ionization, and the specificity of the adsorbent material consisting of MB in solution [52]. Figure 3 graphically shows the effect of pH on the adsorption percentage (%) of MB by the adsorbent consisting of: (A) MTLR, and again of (B) unmodified TLR, at (25±2 °C). The contact time was 45 min, the shaking rate was 170 rpm, and a mass of 500 mg of each of the two adsorbents was used, along with a concentration of 150 mg/l of MB, within a pH range of (3.0–10).

Figure 3 shows that the maximum adsorption percentage for both adsorbents—the MTLR and the unmodified TLR—occurs at a pH of 7.0, reaching approximately 96% and 89%, respectively. The adsorption rate then begins to decrease slightly. The effect of a lower pH (< pH = 7.0) on the adsorption of MB is due to that the protons (H^+) present in the solution can occupy binding sites (active sites), thus reducing and inhibiting the adsorption of MB molecules [53, 54]. Furthermore, MB molecules have a positive surface charge and can repel the protons (H^+) present in the solution, preventing their adsorption by TLR. As the pH increases, the concentration of protons (H^+) in the adsorption solution decreases, weakening the competitive and repulsive interactions, which can lead to an increase in the removal percentage. In general, this high level of adsorption at a pH of 7.0 may be attributed to a positive interaction between certain functional groups present on the surface of the TLR (whether unmodified or chemically modified one), such as amino (-NH2), hydroxyl (-OH) and ether ('R-O-R) groups, with MB dye molecules, as reported elsewhere [55]; these ions with opposite charges are strongly attracted to each other at a pH of 7.0.

3.3 The Effect of the Adsorbents (MTLR & TLR) Dose

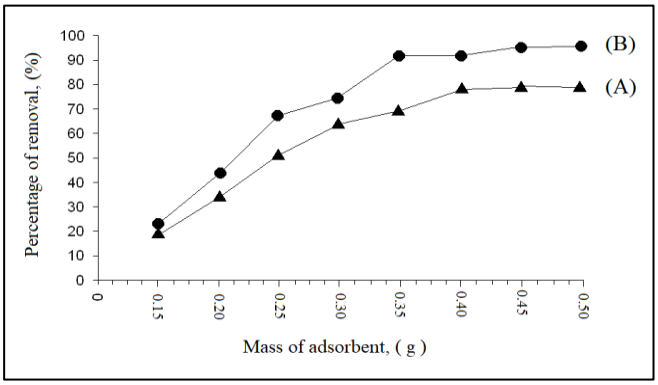


Figure (4): The effect of mass of (A) (TLR) & (B) (MTLR) on removal ratio of (MB).

Figure 4 illustrates the relationship between different masses of raw TLR (Figure 4A) and MTLR (Figure 4B) adsorbents ranging from (1.50–0.50 g) and their effect on the adsorption percentage (%) of MB. These data were obtained from batch adsorption of MB at (25±2 °C), pH of adsorption solution at 7.0, agitation rate of 170 rpm, contact time of 30 min, using a 50 ml solution of 150 mg/l MB concentration.

Figure 4 shows the effect of MTLR mass on MB adsorption. As the residue mass increased, the chemically modified adsorbent exhibited higher efficiency than the unmodified one, with MB adsorption exceeding 95% upon the addition of 0.40 g of the adsorbent. The ratio then stabilized. Therefore, 0.40 g of MTLR was chosen as the optimal maximum dosage of the adsorbent under the operating conditions of this study. The increase in removal percentage of MB molecules with increasing mass of the adsorbent is attributed to the fact that a heavier adsorbent provides a greater number of active sites for adsorption, resulting in a higher removal percentage of the MB, as reported elsewhere [56].

3.5 The Effect of Contact Time

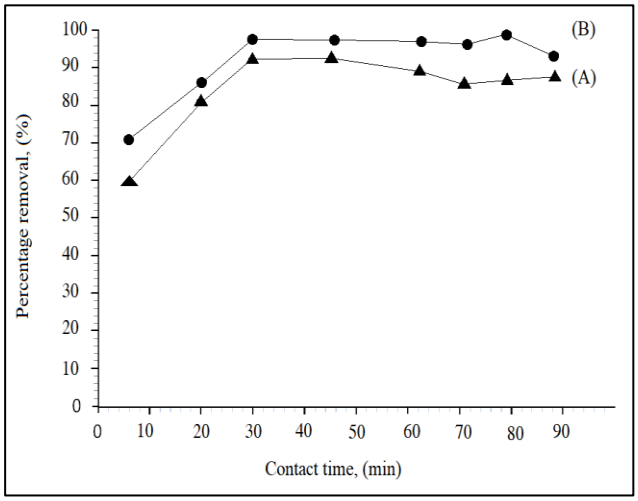


Figure (5): The effect of contact time on adsorption of (MB) by (A) (TLR) and (B) (MTLR).

The adsorption experiments were conducted across various contact times ranging from (5–90 min) at (25±2 °C), a solution pH of 7.0, and a constant adsorbent dosage of 0.40 g for both unmodified TLR and MTLR. Figure 5 illustrates the influence of contact time on the MB removal efficiency (%) at an initial concentration of 150 mg/l for TLR (Figure 5A) and MTLR (Figure 5B). The profiles demonstrate that MTLR consistently exhibits a higher removal efficiency than its unmodified counterpart. Specifically, as the contact time increased from 5 to 90 min, the adsorption efficiency of MTLR rose from 71.98% to 97.3%, while that of TLR increased from 59.21% to 88.47%.

The adsorption rate of MB molecules was highly rapid during the initial 30 min, subsequently slowing down until equilibrium was established. This initial rapid phase is primarily attributed to the abundance of vacant active sites available on the adsorbent surface at the onset of the process. Furthermore, the rapid uptake of MB at a concentration of 150 mg/l indicates that adsorption predominantly occurred on the surface active sites of the MTLR matrix, which aligns with previous findings in the literature [57].

3.2 The Effect of Initial Concentrations of Methylene Blue (MB)

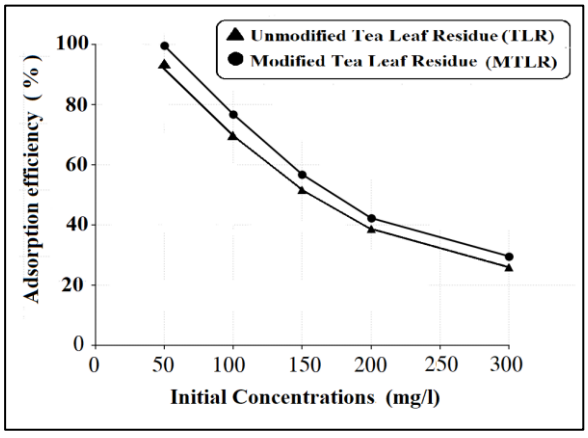


Figure (6): The effect of (MB) concentration on the adsorption efficiency (%) of (MB) by (TLR) and (MTLR).

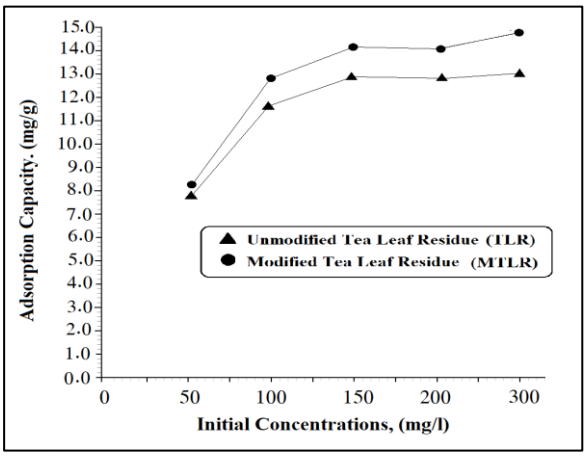


Figure (7): The effect of (MB) concentration on the adsorption capacity (qe) of (TLR) and (MTLR).

Figure 6 illustrates the relationship between the equilibrium concentration (Ce) of the MB adsorbate and its adsorption efficiency (%) using TLR and MTLR. The experimental data were obtained at (25±2 C°), pH 7.0, a contact time of 30 min, and a shaking rate of 170 rpm, using a 0.40 g mass of the adsorbent. **The process was performed in two separate series of experiments: the first utilized MTLR, while the second utilized TLR.** Whereas, **Figure 7** compares the maximum adsorption capacity (q_{max}) of MTLR against TLR as a function of MB concentration.

Figure 6 clearly shows that as the concentration of MB increases from (50−300 mg/l), the adsorption efficiency (%) also increases. It can also be observed that the curve becomes almost linear at a concentration of 150 mg/l for both adsorbents, where any further increase in the concentration of MB has no effect on the removal of either substance from the aqueous medium.

At low initial MB concentrations, the dye molecules were insufficient to occupy the vast number of available active sites, resulting in rapid adsorption by both adsorbents. Conversely, as the initial MB concentration increased, a gradual decrease in the dye removal percentage was observed due to the progressive saturation of these available active sites [58]. Notably, MTLR exhibited a significantly higher adsorption efficiency compared to TLR across all concentration ranges. This enhanced performance is attributed to the chemical modification process, which introduces additional active functional groups and increases the specific surface area, thereby providing more available binding sites for MB molecules [59, 60].

Although higher initial concentrations of MB generally lead to slower overall adsorption kinetics and require longer equilibrium times due to rapid site saturation, they also generate a potent driving force during the initial stages. This concentration gradient effectively overcomes the mass transfer resistance of MB molecules migrating between the aqueous phase and the solid adsorbent surface, consequently accelerating the initial adsorption rate [61, 62].

However, figure 7 illustrates the effect of initial MB concentration on the adsorption capacity at equilibrium (qe). As the initial concentration increases from 50 to 150 mg/l, a sharp enhancement in adsorption capacity is observed due to the high driving force of the concentration gradient. Beyond 150 mg/l, the curves reach a plateau, indicating the saturation of active adsorption sites [63, 64]. From the plot, the optimal experimental adsorption capacity (q_{exp}) is approximately 12.6 mg/g for TLR and 14.1 mg/g for MTLR.

3.6 Isotherm Analysis

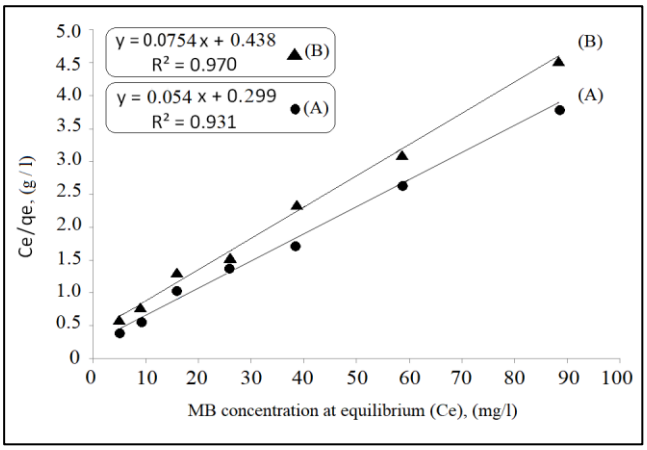


Figure (8): Isotherm equilibrium for the Langmuir linear model of (MB) adsorption on (A) (TLR), and (B) (MTLR).

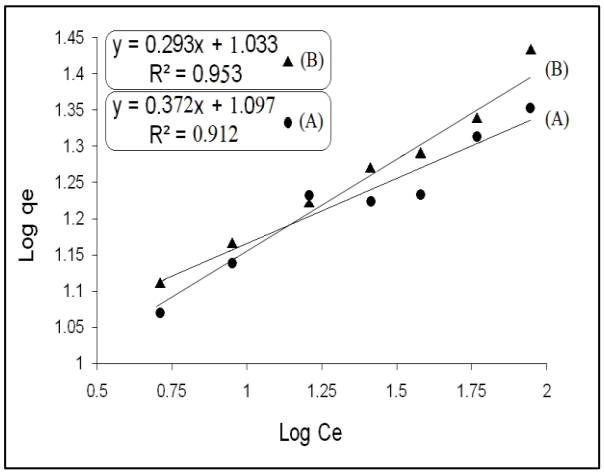


Figure (9): Isotherm equilibrium for the Freundlich linear model of (MB) adsorption on (A) (TLR), and (B) (MTLR).

Linear graphs were obtained using the relationship between (Ce) and (Ce/qe), representing the isotherm equilibrium of the Langmuir model, for the adsorption of MB molecules, first by TLR (Figure 8A) and then by MTLR (Figure 8B). Similarly, linear graphs were obtained using the relationship between (log qe) and (log Ce), representing the isotherm equilibrium of the Freundlich model, for the adsorption of MB molecules, first by TLR (Figure 9A) and then by MTLR (Figure 9B).

The linear regression (R^2) of the Langmuir model was estimated to be approximately 0.970 and 0.931 for adsorption onto MTLR and TLR adsorbents, respectively. In comparison, the linear regression (R^2) of the Freundlich model was estimated to be approximately 0.953 and 0.921 for adsorption onto MTLR and TLR adsorbents, respectively. These values favor the view that the laboratory results agree with the Langmuir model regarding the adsorption of MB onto MTLR. The slope and intercept values obtained from the linear plot were used to determine the maximum theoretical adsorption capacity (q_{max}) and the Langmuir constant (K_L), which reflects the affinity of the binding sites. For the modified adsorbent MTLR, the calculated (q_{max}) and (K_L) values were found to be 13.265 mg/g and 0.1780 L/mg, respectively. To validate the applicability of the Langmuir isotherm model, these theoretical capacities were compared with the experimental equilibrium capacities (q_{exp}).

Interestingly, the theoretical (q_{max}) for MTLR (13.265 mg/g) exhibited a high degree of correlation with its experimental value (14.10 mg/g). Similarly, for the unmodified one of TLR, the calculated Langmuir capacity (q_{cal}) of (10.34 mg/g) was in close agreement with the experimental capacity (q_{exp}) of 12.60 mg/g. This close alignment and minor discrepancy between the theoretical (q_{cal}) and experimental (q_{exp}) values firmly substantiate the suitability and satisfactory fit of the Langmuir model for describing the monolayer adsorption process onto both adsorbents.

Table (2): Results of Langmuir model relating to the adsorption of (MB) by (TLR) and (MTLR), and the Freundlich model relating to the adsorption of (MB) by (TLR) and (MTLR).

Freundlich model adsorption of (MB) by modified tea leaves residues (MTLR)		Langmuir model adsorption of (MB) by modified tea leaves residue (MTLR)	
9.461	K_f (l/g)	13.265	q_{max} (mg/g)
0.153	N	0.178	K_L (l/mg)
0.953	R^2	0.970	R^2
Freundlich model adsorption of (MB) by unmodified tea leaves residue (TLR)		**Langmuir model adsorption of (MB) by unmodified tea leaves residue (TLR)**	
8.458	K_f (l/g)	10.340	q_{max} (mg/g)
0.210	N	0.126	K_L (l/mg)
0.921	R^2	0.931	R^2

4. Conclusion

This study evaluated the efficiency of MTLR via 0.5 M NaOH compared to raw residues for the adsorption of MB. The main findings are summarized as follows:

- **Parametric Influence**: MB adsorption was significantly controlled by adsorbent dose, solution pH, contact time, and initial dye concentration.
- **Alkaline Modification Enhancement**: Alkaline modification via 0.5 M NaOH substantially enhanced the adsorption performance of TLR, **increasing the experimental adsorption capacity (q_{exp}) from 12.60 mg/g for unmodified residues of TLR to 14.10 mg/g for modified residue of MTLR**.
- **Isotherm and Capacity**: The equilibrium data strictly adhered to the Langmuir isotherm model (R^2 = 0.970), yielding a maximum monolayer adsorption capacity (q_{max}) of 13.265 mg/g on the homogeneous surface.
- **Kinetic Behavior**: The adsorption capacity scaled proportionally with initial MB concentrations (50–300 mg/l). The uptake kinetics were initially rapid before slowing down gradually, indicating a surface-controlled attraction mechanism.
- **Sustainability & Recommendation**: Alkaline modification substantially enhanced the adsorption performance of TLR. Given its abundance, eco-friendliness, and cost-effectiveness, this agricultural waste is highly recommended for further exploration in removing other diverse aquatic pollutants beyond MB.

References

[1] Dutta S., Srivastava S., & Kumar C.A., (2021). Recent Advances on the Removal of Dyes from Wastewater Using Various Adsorbents: A Critical Review, *Mater Adv.*, 2: 4497-4531.

[2] Sara D., & Tushar K.S. (2014), Review on Dye Removal from Its Aqueous Solution into Alternative Cost Effective and Non-Conventional Adsorbents, *J. Chem. Proc. Engg.*, 1: 1-11.

[3] Bhardwaj, D., & Bharadvaja, N. (2021). Phyco-Remediation of Effluents Containing Dyes and Its Prospects for Value-Added Products: A Review of Opportunities, *J. Water Process Eng.* 41: 102080.

[4] Katheresan, V., Kansedo, J., & Lau, S.Y. (2018). Efficiency of Various Recent Wastewater Dye Removal Methods: A Review, *J. Environ. Chem. Eng.* 6: 4676–4697.

[5] Semeraro, P., Gabaldon, J.A., Fini, P., Nunez, E., Pellicer, J.A., Rizzi, V., & Cosma, P. (2017), Removal of an Azo Textile Dye from Wastewater by Cyclodextrin-Epichlorohydrin Polymers, IntechOpen: London, UK; ISBN 978-1-78923-069-7.

[6] Srinivasian, A, & Viraraghaven, T., (2010). Decolonization of Dye Wastewater by Biosorption: A Review, *J. Environ. Manage.* 91: 1915-1929.

[7] Pang, Y.I. & Abdullah, A.Z., (2012). Current Status of Textile Industry Wastewater Treatment and Research". Progress in Malaysia: A Review. Clean (Weinh) 41: 751-764.

[8] Sen, T.K., Afroze, S., & Ang, H.M., (2001). Equilibrium, Kinetics and Mechanism of Removal of Methylene Blue (MB) from Aqueous Solution by Adsorption onto Pine Cone Biomass of Pinus Radiata, *Water, Air & Soil Pollution,* 218: 499-515.

[9] Tan, K.L.; & Hameed, B.H. (2017). Insight into the Adsorption Kinetics Models for the Removal of Contaminants from Aqueous Solutions, *J. Taiwan Inst. Chem. Eng.* 74: 25–48.

[10] Elsherif KM, El-Dali A, Ewlad-Ahmed AM, Treban A, & Alttayib I. (2021), Removal of Safranin Dye from Aqueous Solution by Adsorption onto Olive Leaves Powder, *Journal of Materials and Environmental Science*.12(3): 418–430.

[11] Deniz, F., & Karaman, S. (2011), Removal of Basic Red 46 Dye from Aqueous Solution by Pine Tree Leaves, *Chem. Eng. J.*, 170, 67–74.

[12] Miyah Y, Lahrichi A, Idrissi M, Khalil A, & Zerrouq F. (2018), Adsorption of Methylene Blue Dye from Aqueous Solutions onto Walnut Shells Powder: Equilibrium and Kinetic Studies, *Surfaces and Interfaces.*, 11, 74–81.

[13] Xiamin, L., Yang, T., Xiuju, C., Dandan, I., Fang, I., & Wenjing, S., (2008), Preparation and Evaluation of Orange Peel Cellulose Adsorbents for Effective Removal of Cadmium, Zinc, Cobalt, and Nickel, *Colloids and Surface A: Physiochem. Eng. Aspects*, 317, 512–521.

[14] Amjad H. El-Sheikh, Alan P. Newman, Hafid K. Al-daffaee, Suki P., & Neil C. (2004), Characterization of Activated Carbon Prepared from a Single Cultivar of Jordanian Olive Stones by Chemical and Physicochemical Techniques. *J. Anal. Appl. Pyrolysis.,* 71: 151 – 164.

[15] Abudaia, J.A., Al-Ezzaby, K., Al-Shreide, A., & Dawad, E., (2014), Assessments of Activated Carbon Prepared from Date Stones in Adsorption of Indoor Radon, *Al-Nawah Journal*, Tajoura Nuclear Research Center, The Libyan Atomic Energy Establishment, Tripoli-Libya, 11(15): 33 – 42.

[16] Kyzas, G.Z.; Lazaridis, N.K.; & Mitropoulos, A.C., (2012), Removal of Dyes from Aqueous Solutions with Untreated Coffee Residues as Potential Low-Cost Adsorbents: Equilibrium, Reuse and Thermodynamic Approach, *Chem. Eng. J.,* 189–190: 148 – 159.

[17] Nasuha, N., Hameed, B.H., & Din, A.M., (2010), Rejected Tea as a Potential Low Cost Adsorbent for the Removal of Methylene Blue, *J. Hazard. Mater.* 175: 126–132.

[18] Food & Agriculture Organization, FAO. (2022). *International tea market: market situation, prospects and emerging issues*. Rome, Italy.

[19] Hokkanen, S., Bhatnagar, A., & Sillanpää, M., (2016), A Review on Modification Methods to Cellulose-Based Adsorbents to Improve Adsorption Capacity, *Water Research*, 91, 156–173.

[20] Mehmet E. Argun, & Şükrü Dursun, (2006), Removal of Heavy Metal Ions Using Chemically Modified Adsorbents, *J. Int. Environmental Application & Science*, 1(1–2): 27–40.

[21] Ndazi, S., Karlsson, S., Tesha, V., & Nyahumwa, W., (2007). Chemical and Physical Modification of Rice Husks for Use as Composite Panels, *Composites Part A,* 38: 925–935.

[22] Hameed B.H. & Ahmad, A.A., (2009), Batch Adsorption of Methylene Blue from Aqueous Solution by Garlic Peel, an Agricultural Waste Biomass, *J. of Hazardous Materials*, 164, 870–875.

[23] Silvia, A., Jose, L.S., Gabriel, O., & Araceli, R., (2013), Low-Cost Adsorbent for Emerging Contaminant Removal in Fixed Bed Columns. *Chemical Engineering Transactions,* 32: 61–66.

[24] Abbas H.S., Thamer J.M., & Jenan A., (2012), Equilibrium and Kinetics Studies of Adsorption of Metals onto Activated Carbon. *Canadian Journal on Chemical Engineering & Technology,* 3(4): 86–92.

[25] Hairul, N.A., & Kelly, L.K.M., (2011), Adsorption of Basic Red 46 by Granular Activated Carbon in a Fixed Bed Column, *International Conference on Environmental and Industrial Innovation,* 12: *IACSIT Press,* Singpore.

[26] Mall, I.D., Srivastava, V.C., Agarwal, N.K., & Mishra I.M., (2005), Adsorption Removal of Malachite Green Dye from Aqueous Solution by Bagasse Fly Ash and Activated Carbon-Kinetics Study and Equilibrium Isotherm Analysis, *Colloid. Surface.* A, 264(1–3): 17–28.

[27] Danat, B.T., Wuana, R.A., Chahul, H.F., & Saviour, I.M. (2026). Review of Adsorption Isotherms Models, *Applied Water Science,* 16(3), 72–89.

[28] Sevim, F., (2025), Adsorption Capacity, Isotherm, Kinetics, and Thermodynamics Examinations on the Removal of a Textile Azo Dye by Local Natural Adsorbent, *Global Challenges*, 9(5): Art. no. 2500024, doi: 10.1002/gch2.202500024.

[29] Giacomella, A., & Kraiem, N. (2024). Physicochemical characterization and fuel properties of spent coffee grounds and tea leaf residues. *Journal of Analytical and Applied Pyrolysis*, *178*, 106342.

[30] Qiao, H.; Mei, L.; Chen, G.; Liu, H.; Peng, C.; Ke, F.; Hou, R.; Wan, X.; & Cai, H. (2019). Adsorption of Nitrate and Phosphate from Aqueous Solution Using Amine Cross-Linked Tea Wastes, *Appl. Surf. Sci.*, 483: 114–122.

[31] Choudhary, M.; Kumar, R.; & Neogi, S., (2020), Activated Biochar Derived from Opuntia Ficus-Indica for the Efficient Adsorption of Malachite Green Dye, Cu^{+2} & Ni^{+2} from Water, *J. Hazard. Mater,* 392, 122441.

[32] Yasodha, R., Maheswari Patturaj, A., & Samji, A. (2020). Three-Step Identification of Infrared Spectra of Similar Tree Species Using FT-IR Spectroscopy. *Journal of Molecular Structure*, *1218,* 128-134

[33] Mussatto, I.; Machado, S.; Martins, S.; & Teixeira, A. (2011), Production, Composition, and Application of Coffee and its Industrial Residues. *Food Bioprocess Technol.* 4: 661–672.

[34] Oprescu, E.-E.; Enascuta, E.; Vasilievici, G.; Banu, N.D.; & Banu, I. (2022), Preparation of Magnetic Biochar for Nitrate Removal from Aqueous Solutions, *React. Kinet. Mech. Catal.* 135: 2629–2642.

[35] Haafiz, M. K. M., Eichhorn, S. J., Hassan, A., & Javadi, M. (2013). Isolation and characterization of microcrystalline cellulose from oil palm biomass residue. *Carbohydrate Polymers*, *93*(2), 628–634.

[36] Khan, A.; Khuda, F.; Aly, Z.; & Elseman, A.M. (2018), Microwave-Assisted Spent Black Tea Leaves as Cost-Effective and Powerful Green Adsorbent for the Efficient Removal of Eriochrome Black T from Aqueous Solutions, *Egypt. J. Basic Appl. Sci.* 5: 171–182.

[37] Ajay T.T., Nayak, B.B., Martin Xavier K.A., Devangre, A.A., Sandeep B.G., & Amjad K.B., (2023), Phenolic Content and Characterization of Tea Shrub Bottom Leaves, *Agricultural Research Communication Center, (ARCC)*, 43(4): 478-481.

[38] Puziy, M., Poddubnaya, OJ., Martinez-Alonso, A., Suarez-Garcia, F. & Tascon, L.M., (2002). Synthetic Carbons Activated with Phosphoric Acid I. Surface Chemistry and Ion Binding Properties. *Carbon,* 40: 1439-1505.

[39] Rammel, S. & Jamal, M., (2011), "Bio-sorption of Crystal Violet By *Chaetophora Alegans* Algae." *Journal of the University of Chemical Technology and Metallurgy,* 46(3): 283-292.

[40] Ahmed, R., & Kumar, R., (2010), Adsorption Studies of Hazardous Malachite Green onto Treated Ginger Waste. *J. Environ. Sci.,* 91(4): 1032-1038.

[41] Ashly, P, & Thirumalisamy S. (2012), Adsorption of Hazardous Cationic Dyes from Aqueous Solution onto *Acacia Nilotica* Leaves as an Eco Friendly Adsorbent, *Sustain. Environ. Res.,* 22(2): 113-122.

[42] Smith, J. A., & Johnson, R. H. (2021). FTIR spectroscopic Analysis of Cellulosic Matrices. *Journal of Polymer Science*, *59*(3): 123–135.

[43] Sunil K. B., & Arti J., (2012), Equilibrium and Thermodynamic Studies for Adsorption of Crystal Violet onto Spent Tea Leaves, *Water,* 4: 52-71.

[44] Saran S.K.P.; Saritha A.S.; & Sandhya S.S., (2025). FT-IR characterization and Vibrational Analysis of Polyphenolic Compounds in Natural Matrices, *Journal of Molecular Structure*, *1312*, 138450.

[45] Belt, T., & Awais, M. (2024). Characterization of Organosolv Lignins and Cell Wall Structure Using Thermal and FT-IR Spectroscopic Analysis, *Wood Science and Technology*, *58*(5): 1125–1142.

[46] Ren Jian-min., Wu Si-wei, & Jin Wei, (2010), Adsorption of Crystal Violet onto BETA-and CTMA-Bentonite from Aqueous Solutions, *World Academy of Science, Engineering and Technology Journal,* 41: 790-795.

[47] Tounsadi, H.; Khalidi, A.; Abdennouri, M.; & Barka, N., (2015), Biosorption Potential of *Diplotaxis harra L.* and *Glebionis coronaria L.* Biomasses for the Removal of Cd(II) and Co(II) from Aqueous Solutions, *J. Environ. Chem. Eng.*, 3, 822–830.

[48] Malkoc, E.; & Nuhoglu, Y., (2006), Removal of Ni(II) Ions from Aqueous Solutions Using Waste of Tea Factory: Adsorption on a Fixed-Bed Column, *J. Hazard. Mater.*, 135, 328–336.

[49] Seema Patel, (2012). Potential of Fruit and Vegetable Wastes as Novel Biosorbents: Summarizing the Recent Studies, *Reviews in Environmental Science and Bio/Technology,* 11:(4), 365-380.

[50] Ahmad, A., Khan, S., & Rahman, F. (2024). Mechanistic Insights into Methylene Blue Adsorption onto Modified Biomass Matrices: Role of Chemisorption and Electrostatic Interactions. *Journal of Environmental Chemical Engineering*, 12(2): 111820.

[51] Kyzas, G. Z., & Mitropoulos, A. C. (2025). Advanced Functional Materials for Dye Immobilization: Surface Functional Groups and Binding Mechanisms. *Colloids and Surfaces A: Physicochemical and Engineering Aspects*, 681, 132740.

[52] Kołodynska, D.; Wnetrzak, R.; Leahy, J.J.; Hayes, M.H.B.; & Hubicki, Z. (2012), Kinetic and Adsorptive Characterization of Biochar in Metal Ions Removal, *Chem. Eng. J.* 197, 295–305.

[53] Zhao,L.; Yang, S.T.; Feng, S.; Ma, Q.; Peng, X.; & Wu,D. (2017), Preparation and Application of Carboxylated Graphene Oxide Sponge in Dye Removal, *Int. J. Environ. Res. Public Health*, 14, 1301.

[54] Ma,L.; Jiang, C.; & Zou, Z. (2018), Microwave-Hydrothermal Treated Grape Peel as an Efficient Bio-sorbent for Methylene Blue Removal, *Int. J. Environ. Res. Public Health*, 15, 239.

[55] Singh, R., Singh, T.S., Odiyo, J.O., Smith, J.A., & Edokpayi, J.N., (2020), Evaluation of Methylene Blue Sorption onto Low-Cost Bio-sorbents: Equilibrium, Kinetics, and Thermodynamics, *Journal of Chemistry*, Art. no. 8318049.

[56] Jaramillo-Fierro, X., & Cuenca, G. (2024), Theoretical and Experimental Analysis of Hydroxyl and Epoxy Group Effects on Graphene Oxide Properties, *Nanomaterials*, 14(8): https://doi.org/10.3390/NANO14080714/S1

[57] Oliveira, L.S., Franca, A.S., Alves, M., & Rocha, F. (2008), Evaluation of Untreated Coffee Husks as Potential Bio-sorbent for Treatment of Dye Contamination Water. *J. Hazard. Mater.* 155: 507–512.

[58] Hassan, W.; & Khan, M.A.; (2017), Potential Bio-sorbent, Haloxylon Recurvum Plant Stems, for the Removal of Methylene Blue Dye, *Arabian Journal of Chemistry*, 10, 1512–1522.

[59] Al-Zoubi, H., Al-Amr, A., & Hussein, M. A. (2025). Optimized removal of Methylene Blue from Wastewater Using Ammonia-Doped Composite Materials: Role of Enhanced Specific Surface Area and Active Functional Groups. *Scientific Reports*, *15*(1), 8783.

[60] Ogedengbe, K. O., Ayodele, O. S., & Babalola, J. O. (2024). Functionalized Bioadsorbent Application on Methylene Blue Removal: Systematic Study on Surface Area Enhancement and Chemical Agents Influence. *International Journal of Chemical Engineering*, 2024, Art. no. 5704096.

[61] Stjepanovic, M.; Velic, N.; & Habuda-Stanic, M. (2022). Modified Hazelnut Shells as a Novel Adsorbent for the Removal of Nitrate from Wastewater, *Water*, 14, 816.

[62] Liu, Q.; Deng, W.-Y.; Zhang, L.-Y.; Liu, C.-X.; Jie, W.-W.; Su, R.-X.; Zhou, B.; Lu, L.-M.; Liu, S.-W.; & Huang, X.-G. (2023), Modified Bamboo Charcoal as a Bi-functional Material for Methylene Blue Removal, *Materials*, 16, 1528.

[63] Zhao, M., & Liu, P., (2008), Removal of Methylene Blue from Aqueous Solution with Silica Nanosheets Derived from Vermiculite. *Journal of Hazardous Materials*, 158: 43.

[64] Dogan, M., Abak, H., & Alkan, M., (2009), Adsorption of Methylene Blue onto Hazelnut Shell: Kinetics, Mechanism and Activation Parameters, *Hazard. Mater. J.*, 164: 172.